Control of Prosumer Networks

Nicolas Gensollen, Monique Becker, Vincent Gauthier and Michel Marot
CNRS UMR 5157 SAMOVAR,
Telecom SudParis/Institut Mines Telecom
Email: {nicolas.gensollen, vincent.gauthier, michel.marot, monique.becker}@telecom-sudparis.eu

Abstract—The ability to control a given network by dynamically injecting inputs offers ways to make sure that it stays in stable regions. In the case of smart grids, where end users exhibit complex behaviors and renewable production is quite unstable, control of the system is paramount. In this paper, we study the case of a network composed of entities called prosumers. These agents have the ability to both consume and produce according to external conditions. We first model and simplify the underlying dynamic of such network using a second order coupled oscillators network model. Under some conditions, the system synchronize to a common frequency. However, in case of perturbations in the power distribution, the system might lose synchrony and require control to bring it back to the stable state. In this situation, control can be seen as energy absorbed or injected in the system at specific locations. Moreover, the power outputs of the prosumers are susceptible to change such that loads and generators are not fixed. In this context, it is important to select the right subset of nodes that yields, on average, the cheapest control in terms of energy.

I. Introduction

Modernizing the power grid and increasing the share of renewables in the production are substantial objectives of the energetic transition. Because of progresses in communication, data management, and storage, the upcoming emergence of a power grid "2.0", often called smart grid, appears as a cross-disciplinary challenge of the 21st century [1].

The today centralized top-down architecture is set to evolve to more distributed and bi-directional systems. Furthermore, the emergence of renewable and stochastic distributed energy resources (DER) in the distribution networks will require more flexibility. All these evolutions might change deeply the ways end users perceive and consume electricity. The consumer of the future, while seeking maximum utility/profit tradeoffs, is expected to be more involved in the system operation. Using dynamic signals such as real time electricity prices for instance, load curves could be shaped to some extend as to agree with the production conditions of the grid. Within these complex systems with numerous agents, it is assumed that multiple aggregation levels will be required in order to organize and optimize communication. Agents responsible for generation and load portfolio managment, i.e prosumers [2], will provide services (generation, load shedding, frequency regulation) against remuneration. Insure grid stability within this uncertain context appears as a complex task.

Several studies highlighted the need for increasing the storage capacity of the system. Some of them even consider electric vehicles as moving capacities that could be used for frequency regulation. In the case of fixed storage devices, the locations where they should be installed is an important question since it impacts the performances of the system. In a very static and top-down architecture, where loads and generators are fixed, this question is far from trivial. But in a smart grid scenario with bi-directional flows and agents that produce and consume depending on weather conditions, this becomes even more challenging. In this paper, we explore the use of storage in a network of prosumers whose power outputs are susceptible to change due to various external causes.

More precisely, we model the power grid as a coupled oscillator network, where each node is represented as an oscillator with a phase angle and a natural frequency that are impacted by the ones of their neighbors. Since the work of Kuramoto [], networks of coupled oscillators have been used to model various phenomenons such as fireflies, ex2, or power grids. Indeed, it is well-known that synchronization of all rotating elements to a common frequency is necessary within a power grid for stable operation. Inspired by [3], we use a second order Kuramoto model in order to obtain a simplified dynamics for the power grid (see Section II).

We will see that under some conditions, the system synchronizes to a common frequency Ω. However, this synchronized state is suceptible to break if perturbations occur. If, for example, the production of some generator decreases while the load remains the same, the imbalance between production and consumption might steer the frequency away from Ω and drive the system to unstable conditions. These kinds of perturbations are very likely in a scenario with high penetration of DER. Multiple control techniques, with different time scales, exits in order to cope with such events. Among others, it has been argued that storage and vehicle to grid (V2G) technology could be used for frequency regulation. If a sudden drop or raise of the frequency due to an imbalance is detected, some devices are charged or discharged as to restore synchrony. This approach poses a few questions such as the location of the storage devices, or the quantities of power that should be injected or absorbed. Since charging and discharging a battery is costly, we are particularly interested in the energy necessary to restaure synchrony. Moreover, in a prosumer scenario where generators and loads tend not to be fixed, we would like to find a subset of locations for installing storage such that the energy is low on average.

We will see that these storage actions can be interpreted as an additional term in the oscillators dynamics for a subset of nodes. We propose here to use complex network control theory [4] in order to model the impact of the storage equipments

on the network dynamics (see Section III). Placing storage at some node can thus be seen as selecting this node in the driver set, such that finding the locations for the storage devices could be related to finding the driver set of the network. Nevertheless, selecting the drivers that, on average, will control the network with low energy is a hard problem. Recent studies showed though the existence of relationships between controllability and submodular set functions [5]. These functions, that we introduce in more depth in section X, have the interesting property of having diminishing returns as we increase the size of the set considered. Although finding the optimal set is NP-hard, [6] proposed a simple greedy algorithm with a worst case guaranty.

Since the system under study is a power grid which lines and batteries have finite capacities, we have further constraints on the control signals. Obviously, no line can be overloaded while trying to restaure synchrony. Likewise, no battery can inject power when empty, or charge/discharge quicker than some maximum rate. We propose here to incorporate these constraints in the search of the driver set (see section IV).

This paper is organized as follows, section II presents the oscillator model used for simplifying the grid's dynamics. Section 3 introduces submodular functions and their maximization. Section 4 gives basic notions of control theory and links controllability to submodular set functions. In section IV we develop the constraints relative to the system and the batteries. Finally, in section V, we show some results.

II. THE MODEL

In this section, we introduce the coupled oscillators network model used to simplify the power grid dynamic. The detailed derivation of the second order dynamics can be found in [3], and the key points are reproduced here for the convenience of the reader.

The objective is to achieve synchronization of the grid at the main frequency $\Omega = 50Hz$. Each oscillator i has a phase angle δ_i and a frequency $\dot{\delta}_i$. Therefore, we seek an equilibrium of the form : $\forall i,\ \dot{\delta}_i = \Omega$. For convenience, we express the dynamic of the oscillators in terms of the deviations from the main frequency : $\delta_i(t) = \Omega t + \theta_i(t)$. Let $\omega_i = \dot{\theta}_i$, such that $\dot{\delta}_i = \Omega + \omega_i$. The equilibrium, in terms of the deviations dynamics, is : $\forall i,\ \omega_i = 0$

The next step consists in translating the dynamics of the generators and machines into equations involving the phase angles θ_i and the frequencies ω_i. Generators and machines are composed of a turbine that dissipates energy at a rate proportional to the square of the angular velocity ($P_{diss} = FV \sim V^2$) :

$$P_{diss,i}(t) = K_{Di}(\dot{\delta}_i(t))^2 \qquad (1)$$

where K_{Di} is the dissipation constant of entity i.
Furthermore, it also accumulates kinetic energy at a rate :

$$P_{acc,i}(t) = \frac{1}{2}I_i\frac{d}{dt}\left(\dot{\delta}_i(t)^2\right) \qquad (2)$$

where I_i is the moment of inertia of entity i. For simplicity, we consider that all entities have the same dissipation constants(K_D) and moment of inertia (I).

The condition for the power transmission between i and j is that the two devices do not operate in phase : The phase difference between i and j is : $\delta_j(t) - \delta_i(t) = \Omega t + \theta_j(t) - \Omega t - \theta_i(t) = \theta_j(t) - \theta_i(t)$. The transmitted power along the line can be written as :

$$P_{transmitted} = -P_{ij}^{MAX}sin(\theta_j - \theta_i) \qquad (3)$$

with P_{ij}^{MAX} being the maximum capacity of the line (i, j). If i is connected to more than one other entities, this equation becomes ($\mathcal{N}_i$ being the neighborhood of i) :

$$P_{transmitted} = -\sum_{j\in\mathcal{N}_i} P_{ij}^{MAX}sin(\theta_j - \theta_i) \qquad (4)$$

Each entity i is then described by a power balance equation of the type :

$$P_{S,i} = P_{diss,i} + P_{acc,i} + P_{transmitted,i} \qquad (5)$$

By substituting and re-arranging the terms, we obtain the following non-linear coupled system of equations :

$$P_{S,i} = I\Omega\ddot{\theta}_i + \left[I\ddot{\theta}_i + 2K_D\Omega\right]\dot{\theta}_i + K_D\Omega^2$$
$$+K_D\dot{\theta}_i{}^2 - \sum_{j\in\mathcal{N}_i} P_{ij}^{MAX}sin\left[\theta_j - \theta_i\right] \qquad (6)$$

We now use simplifications based on the fact that we consider small deviations from the main frequency : $\dot{\delta}_i \sim \Omega$ which means that $\omega_i = \dot{\theta}_i << \Omega$, such that the squared term $K_D\dot{\theta}_i^2$ can be neglected. Moreover, we assume that the rate at which energy is stored in the kinetic term is much less of the rate at which energy is dissipated by friction : $\ddot{\theta}_i << \frac{2K_D}{I}$ (see [3] for more details). Equation 6 becomes :

$$\ddot{\theta}_i \sim \psi_i - \alpha\dot{\theta}_i + \sum_{j\neq i} K_{ij}g_{ji}sin\left[\theta_j - \theta_i\right] \qquad (7)$$

Where $\alpha = \frac{2K_D}{I}$ is the dissipation term, $K_{ij} = \frac{P_{ij}^{MAX}}{I\Omega}$ are the coupling strengths, $\psi_i = \left[\frac{P_{S,i}}{I\Omega} - \frac{K_D\Omega}{I}\right]$, and g_{ij} is the coefficient of the adjacency matrix G. By working in a rotating frame, we can simplify $\psi_i = \frac{P_{S,i}}{I\Omega}$.

The dynamic is still non linear because of the sine coupling. Therefore, we also assume that the phase angle differences are small such that $sin\left[\theta_j - \theta_i\right] \sim \theta_j - \theta_i$. By using vector notations, the dynamic can be written in the following form :

$$\ddot{\theta} = \Psi - \alpha\dot{\theta} - KL\theta \qquad (8)$$

Where L is the Laplacian matrix of the underlying topology (k_i is the degree of node i):

$$L_{ij} = \begin{cases} k_i & if\ i = j \\ -g_{ij} & if\ i \neq j \end{cases} \qquad (9)$$

Equation 8 is a continuous time second order linear system of N equations. We first transform this into a continuous time

first order linear system of $2N$ equations by introducing the following vector : $X = \begin{pmatrix} \theta \\ \dot{\theta} \end{pmatrix}$:

$$\dot{X} = \begin{pmatrix} 0 & I \\ -KL & -\alpha I \end{pmatrix} X + \begin{pmatrix} 0 \\ \Psi \end{pmatrix} \qquad (10)$$

Which can be written in discrete time:

$$X(t + \Delta t) = MX(t) + \begin{pmatrix} 0 \\ \Psi \Delta t \end{pmatrix} \qquad (11)$$

With $M = \begin{pmatrix} I & I\Delta t \\ -KL\Delta t & (1 - \alpha \Delta t)I \end{pmatrix}$.

By setting $Y(t) = \begin{pmatrix} X(t) \\ 1 \end{pmatrix}$, let the dynamic be :

$$Y(t + \Delta t) = AY(t) \qquad (12)$$

With transition matrix A :

$$A = \begin{pmatrix} I & I\Delta t & 0 \\ -KL\Delta t & (1 - \alpha \Delta t)I & \Psi \Delta t \\ 0 & 0 & 1 \end{pmatrix} \qquad (13)$$

Equation 12 is a linear discrete time system of $2N + 1$ equations. Note that the transition matrix A encodes all the system parameters, topology, and power distribution.

III. CONTROL AND SUBMODULARITY

A. Submodularity

In this section we provide a very brief introduction to what submodular functions are, and how their maximization could be achieved in reasonable time. More information can be found in [7].

A set function $F : 2^V \longrightarrow \Re$ defined over a finite set V is said to be submodular if it satisfies :

$$\forall S, T \in V, \ F(S) + F(T) \geq F(S \cup T) + F(S \cap T) \quad (14)$$

Another equivalent definition is that for all sets $X, Y \in V$, such that $X \subseteq Y$ and for all element $x \in V \setminus Y$,

$$F(X \cup \{x\}) - F(X) \geq F(Y \cup \{x\}) - F(Y) \qquad (15)$$

This basically means that submodular functions exhibit a diminishing return property which makes them particularly interesting for optimization. A very intuitive example is the optimum placement of sensors in an area (see figure **??**). Sensors can be placed on a grid of locations and function F computes the surface of the space that is being sensed. Note first that adding a new sensor i to the current set S cannot decrease the value of F : $F(S + \{i\}) >= F(S)$. Furthermore, if we add sensor i to a small set S_1 we tend to get larger improvements than if we add i to a larger set $S_2 \supset S_1$.

Finding the set S_k of size k that maximizes a set function F is a difficult problem because the number of sets grows exponentially with the number of nodes. Therefore complete enumeration and evaluation is only a feasible solution on very small examples. Nevertheless, if the set function is
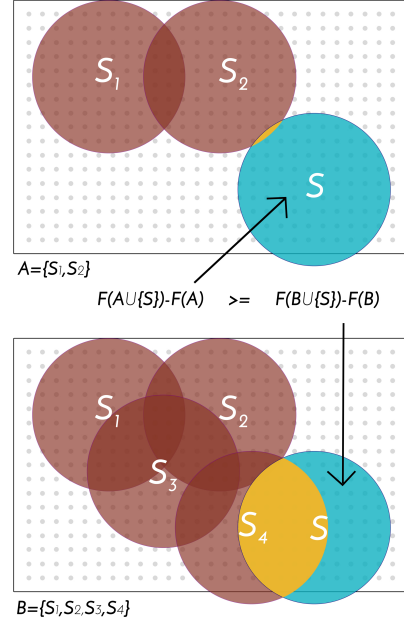

Figure 1: Submodularity example with sensor placements.

submodular, a simple greedy heuristic returns a solution $S_k^\star$ such that, in the worst case, $\frac{F(S_k^\star)}{F(S_k^{OPT})} \sim 63\%$ (where S_k^{OPT} is the optimum set of size k) [7]. This heuristic starts with a set S (possibly empty) and add the element i that exhibits the highest marginal gain : $F(S \cup \{i\}) \geq F(S \cup \{j\}) \ \forall j$.

For a ground set of N elements, this heuristic computes F $\frac{k(2N-k+1)}{2}$ times. Since the evaluation of F can be costly, a well-known lazy-greedy variation has been proposed by [6]. This smart implementation uses the submodular structure of the marginal gains in order to reduce the number of calls to F. This requires to maintain a sorted table of marginal gains for all elements. When looking for new element i to add to set S, the top one is selected and the new marginal gain $F(S \cup \{i\}) - F(S)$ is computed. If this gain is larger than the gain of the second element in the table, then i is added to S. Otherwise i is inserted back in the table with its updated gain and the same treatment is applied to the element that is now on the top of the table. Because of the submodularity of F, this method performs as well as the original one, but can result in speedups of several order of magnitudes.

B. Control

In this section, we introduce basic tools from control theory and relate them to the submodular functions introduced above.

We assume the control of a subset of the nodes that we call driver nodes. In our particular power grid situation, a driver node can be seen as a prosumer where some additional storage equipment is used to inject or absorb energy from the system. The dynamics of equation 12 becomes :

$$Y(t + \Delta t) = AY(t) + Bu(t) \qquad (16)$$

Where the control matrix B is an indicator of the driver nodes, and $u(t)$ represents the control vector input at time t. The system is said to be controllable in T steps if it can be steered from any initial state Y_0 to any final state Y_f through a sequence of control inputs $u(t)$.

Controllability in complex network became popular with the well-known structural controllability framework introduced by Lin [8]. This approach relates the search of the minimum driver set to a maximum matching in a bipartite graph, which can be done with the Hopcroft-Karp algorithm in $O(|E|\sqrt{|V|})$ in the worst case. This requires that the system (A, B) is a structured system, meaning that all elements in A and B are either fixed zeros or independant free parameters. In such a situation, structural control is extremely powerfull since it enables us to discuss a network's controllability relatively quickly even if we do not know the exact weights of the edges. Note however that the independance of the parameters is a key assumption. If A is the adjacency matrix of an undirected network for instance, independance is not true since A is symetric, and one must use different tools to study controllability [9].

On the other hand, if the system is controllable, there might be more than one sequence of control inputs $u(t)$ that could drive it from Y_0 to Y_f. Among all these possibilities, optimal control is devoted to find the sequence that minimize some cost function that can depend on the sates of the system $Y(t)$, the control inputs $u(t)$, and the final state $Y(T)$. As explained above, we are interested in the sequence that requires the minimum amount of control energy [10]. Let $\mathcal{E} = \int_{t_0}^{t_0+T} \|u(t)\|^2 dt$ be the energy used for the control of the system. It can be shown [4] that the control input sequence that minimizes the control energy can be written as :

$$u^\star(t) = B^T (A^T)^{T-t-1} W^{-1}(T) \nu(T) \qquad (17)$$

where $\nu(T) = Y_f - A^T Y_0$ is the difference between the desired final state and the final free state, and $W(T) = \sum_{k=0}^{T} A^k BB^T (A^T)^k$ is called the Gramian matrix of the system. It can be shown that the system is controllable if and only if the Gramian is not singular, and that its rank indicates the dimension of the controllable subspace. Besides, the minimum control energy associated with the inputs $u^\star(t)$ can be written as :

$$\mathcal{E}_{min} = \nu(T)^T W^{-1}(T) \nu(T) \qquad (18)$$

In cases where W is not invertible, the pseudo-inverse $W^\dagger$ can be used to obtain similar information in the controllable subspace. The last row of matrix A in equation 16 adds a dimension to the state space that does not correspond to any phase angle or frequency but makes W singular. Since we seek control in the first $2N$ dimensions, we will use $W^\dagger$ in practice, and consider full control of the system if $rank[W] = 2N$.

Not surprisingly, $\mathcal{E}_{min}$ depends on the initial and final states as well as on the inverse of W which only depends on A and B. The gramian can thus be used to obtain information about average controllability in the state space. In the prosumer network that we consider, generators and loads (Ψ) are suceptible to change, meaning that initial (Y_0) and final (Y_f) states might also vary. In such a scenario, we prefer to aim at good performances on average, rather than very good performances in few specific cases and bad performances in all other situations.

Since the control energy is related to W^{-1}, systems with "large" W will tend to be controlled with low energy. Still, this notion of "large" W is not very accurate and we need to quantify it by taking some metric based on W. We already mentioned the rank of W as being the dimension of the controllable subspace, but it is also known that the trace of W and W^{-1} give information about average controllability and average control energy [5]. In such a situation, we can build a set function that, given a set of driver nodes S, returns the value of one of these metrics. Indeed, given A and S, we can obtain the system dynamics (A, B_S) and compute the gramian W_S. In other word, such a function would quantify the ability of a given set of nodes to contol the system on average.

A key point, demonstrated in [5], is that the set function $F : S \longrightarrow Tr[W_S]$ is modular and the two functions $F : S \longrightarrow Tr[W_S^{-1}]$ ans $F : S \longrightarrow rank[W_S]$ are submodular. This nice result enables us to look for the driver node set that optimizes some notion of the average controllability using a simple greedy heuristic with a worst case guarantee (see section X).

Theoretically, we are now able, for a given prosumer network, to compute A, B, and W. For some trajectory in the state space, we can use equation 17 to find the optimum control inputs. However, since we are considering a power grid as a network, we would like to verify that these inputs will ensure that the system physical constraints are respected in the process. We propose in the next section to take into account constraints related to line capacities and storage imperfections.

IV. CONTROL OF THE PROSUMER NETWORK

A. Flow Constraints

The power transmitted on line (i,j) is $P_{i \longrightarrow j} = -P_{ij}^{MAX} (\theta_j(t) - \theta_i(t))$. Flow constraints at time t can thus be written as :

$$\forall (i,j) \in V^2, \quad g_{ij} \mid \theta_j(t) - \theta_i(t) \mid \leq 1 \qquad (19)$$

If these constraints are verified for all instants t during the control phase then no line gets overloaded by the action of the control inputs.

[11] showed that a condition for synchronisation in a coupled oscillators network is $\|L^\dagger \omega\|_\infty \leq sin(\gamma)$, where L is the Laplacian matrix of the network, ω is the vector of the natural frequencies of the oscillators, and $\|x\|_\infty = max |x_i - x_j|$. If this condition is satisfied, the oscillators synchronize at the common frequency ω_{SYNC} with the phase lock $g_{ij} |\theta_i - \theta_j| \leq \gamma \in [0, \frac{\pi}{2}], \forall (i,j) \in V^2$. The synchronisation condition becomes in our settings :

$$\| \left(L \circ P^{MAX} \right)^{\dagger} \Psi \|_{\infty} \leq sin(1) \qquad (20)$$

Where $A \circ B$ represents the Hadamard product between matrices A and B. If constraint 20 is satisfied, the oscillators synchronize to a common frequency $\omega_{SYNC} = \frac{\sum_{k=1}^{N} \Psi_k}{\sum_{k=1}^{N} \alpha_k} = \frac{\sum_{k=1}^{N} P_{S,k}}{I\Omega N \alpha}$.

Since the dynamics is expressed in term of deviations from Ω, synchronization at Ω is achieved if $\omega_{SYNC} = 0$. Wich gives the production consumption balance constraint :

$$\sum_{k=1}^{N} P_{S,k} = 0 \qquad (21)$$

Constraints 20 and 21 ensure that the system is able to synchronize at Ω without overloading lines.

B. Battery Constraints

As for power lines, we need to take into account the imperfections of the storage that we consider. In practice, we could use some detailed and complex models, but as to keep things simple, we adopt here a straightforward approach. A storage i has a maximum charge/discharge rate r_i, some amount of energy stored at time t $\Lambda_i(t)$, and a maximum capacity $\Lambda_{i,MAX}$. We assume that all maximum rates (r) and all maximum capacities Λ_{Max} are the same accross the storage equipments. We also denote by $\Lambda(t)$ the vector of energy level at time t. Since $u^{\star}(t)$ specifies the control inputs, the energy level dynamic of the batteries is $\Lambda(t+\Delta t) = \Lambda(t) - u^{\star}(t)I\Omega$. Which can also be written as :

$$\Lambda(t) = \Lambda(0) - I\Omega \sum_{k=0}^{t} u^{\star}(k) \qquad (22)$$

Where $\Lambda(0)$ is the vector of initial levels in the batteries. Obviously, $\Lambda(t)$ has to stay within possible bounds : $\forall t, \quad 0 \leq \Lambda(t) \leq \Lambda_{MAX}$. Which can be written in terms of the control inputs :

$$\forall t, -\frac{\Lambda(0)}{I\Omega} \leq -\sum_{k=0}^{t} u^{\star}(k) \leq \frac{\Lambda_{MAX} - \Lambda(0)}{I\Omega} \qquad (23)$$

Finally, during each time slot, the battery cannot charge or discharge at a rate higher than r :

$$\forall t, \quad | u^{\star}(t)I\Omega | \leq r \qquad (24)$$

C. Algorithm

We propose the following greedy algorithm in order to find the smallest set of locations that minimizes the average control energy and satisfy the constraints. We assume here that the system is in a given initial state Y_0 and we want to reach a desired final state Y_f in T time steps. The algorithm 1 starts with an empty set and, as long as that constraints are not satisfied, it increases the size of the set. For a given size k, the set S_k is found using lazy greedy submodular optimization of a Gramian-based set function F. In practice

we use $F(S) = -Tr\left[W_S^{\dagger}(T) \right]$ which quantifies the average energy required to move the system around the controllable subspace. The algorithm 1 returns then the tuple $(k, S_k, u^{\star})$ such that S_k is the smallest set that minimizes the average control energy and, in this case, satisfies the constraints with control $u^{\star}$.

Algorithm 1 Greedy submodular optimization with constraints

---

while Not $\begin{cases} rank\left[W_{S_k}(T) \right] < 2N \; and \\ \forall t, \forall (i,j) \in V^2, g_{ij} \, |\theta_j(t) - \theta_i(t)| \leq 1 \; and \\ \forall t, -\frac{\Lambda(0)}{I\Omega} \leq -\sum_{k=0}^{t} u^{\star}(k) \leq \frac{\Lambda_{MAX} - \Lambda(0)}{I\Omega} \, and \\ \forall t, \; |u^{\star}(t)| \leq \frac{r}{I\Omega} \end{cases}$

do

$\quad k \qquad \leftarrow k + 1$
$\quad S_k \qquad \leftarrow Subopt(F, k)$
$\quad u^{\star}(t) \qquad \leftarrow OptControl(S_k)$

end while

V. RESULTS

We first consider a small example of 10 nodes connected with an erdos-renyi topology. The power distribution and the capacities of the lines are selected randomly such that the system is at equilibrium. Therefore, the production matches the consumption, no line is overloaded and all nodes are synchronized to the main frequency. We use the greedy algorithm 1 based on the trace of the inverse Gramian as to select the driver set S. At a given time t_k, we introduce a small perturbation in the form of a mismatch between the production and consumption : $P_i(t_k) = P_i(t_{k-1}) + \delta P$ for some random node i. Consequently, the frequencies $\dot{\theta}_i \forall i$ of the oscillators start to deviate from the synchronized state. At time $t_k + d$, we apply to the drivers the optimal control of equation 17 such that the system is brought to the synchronized state at time $t_k + d + T$, where T is the control time. At this time, if the mismatch between production and consumption is still active, we maintain synchrony by using optimal control with $T = 1$. Figure 2 shows the evolution of the nodes' frequencies during the control phase.

The purpose of selecting the drivers according to a Gramian related metric is to minimize, on average, the amount of control energy needed. In other words, if we select the drivers randomly, we expect to need, on average, more energy to control the system. In figure 3, we draw 10^4 example systems of 50 nodes with random scale-free topologies (Barabasi-Albert model is used), and random power distributions and line capacities. For each system we select a random number of drivers $N_D \sim \mathcal{U}(1, N_{nodes})$ and we find two driver sets of size N_D. One is chosen randomly and the other is found with algorithm 1. For both sets, we draw a random initial state Y_i and a random final state Y_f, and we compute the control energy required for driving the system from Y_i to Y_f. On figure 3 we plot each system as a dot with coordinates $(n_D = N_D/N_{nodes}, log(\mathcal{E}))$. The color indicates what method has been used, and the lines show the average accross n_D. As visible, both curves decrease as the number of drivers increases, meaning that, as the number of drivers grows, the
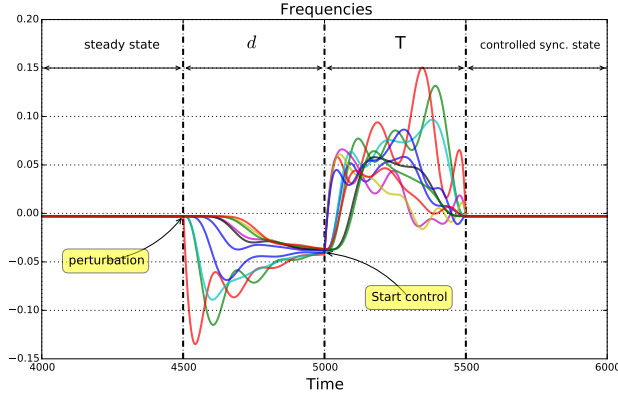
Figure 2: Time series of the N frequencies ω_i (phase angles are not shown for clarity). d is the delay between the perturbation and the begining of the control phase that bring the system bak in the synchronized state in T time steps. Here, d was chosen quite large for the clarity of the figure. Note that, if the perturbation is still active at this point, the system still needs control in order to stay synchronized (batteries should still compensate the power imbalance)

Figure 3: Control energy $log(\mathcal{E})$ against size of control set n_D for random and optimized driver sets. Topologies are drawn from a Barabasi-Albert model with $N_{nodes} = 50$, power and line capacity distributions are random. For both case, 10^4 instances are considered and the results are displayed as dots. The lines shows the average for both case.

average control energy tends to decrease. Furthermore, we tend to use, as exected, less energy when the drivers are carefully selected. Note that this difference tends to zero when n_D tends to one, because almost all nodes are then selected, yielding little flexibility for optimization.

We investigate next how the topology of the grid affects the size of the control set. We consider first the case of an erdos renyi topology with probability of connection p. We show on Figure 4 how the size of the driver set evolves with p for different Gramian based metrics and for two levels of constraints :

- Level 1 : full control : the system can be moved from any point to any other point of the state space. We do not consider constraints on the energy which can tend to infinity.
- Level 2 : full control + line capacities constraints + battery constraints (see algorithm 1). This level is much more demanding since we impose the ability to move the system from any point to any other point, without overloading any line or breaking any battery limits in the process.

When p is close to zero, nodes tend to be very poorly connected such that we need to control almost all nodes in the grid. As p increases, the connectivity of the graph augments and the number of drivers decreases. At some point, the connectivity of the graph starts to harm its controllability, and more drivers are needed. This effect is in accordance with the litterature although it is less marked here because the topology has less influence in our model (recall that matrix A in the dynamics is not the adjacency matrix of the graph but a block matrix where one of the block is the Laplacian
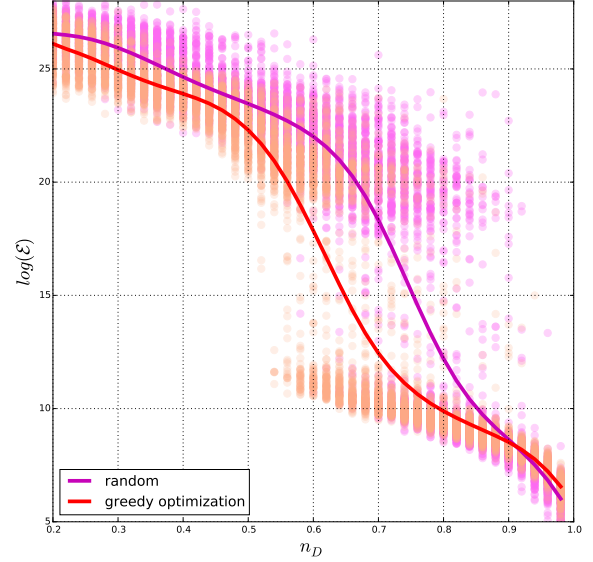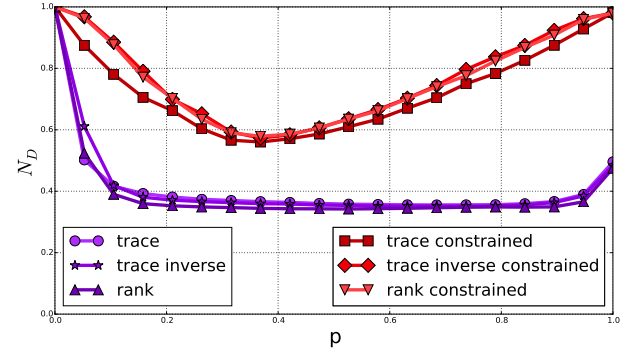

Figure 4: n_D against link probability p for erdos-renyi topologies ($N = 100$). Curves are averaged over 100 realizations. The top three curves show the results for the three metrics taken into consideration when all constraints are considered (see Level 2 in the main text). The bottom three curves exhibit the results for the same metrics when only the full controllability constraint is considered (see Level 1 in the main text).
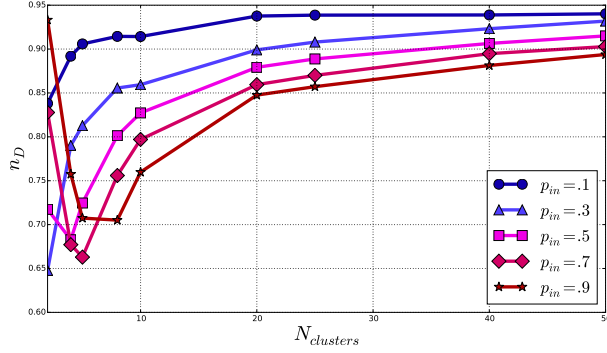
6

Figure 5: n_D against $N_{clusters}$ for different values of p_{in} and $p_{out} = 0.1$. $N = 200$ and curves are averaged over 100 realizations.

Figure 6: n_D against p_{in} for systems of $N = 200$, $p_{out} = 0.1$, and for different values of $N_{clusters}$. The curves are averaged over 100 realizations.

matrix of the graph). As expected, the driver sets for the level 2 of constraints are larger than for level 1 (for all metrics) because we impose far more constraints.

Because transmission power grids are spatially and politically constrained (each contry has its own transmission grid which is interconnected with neighboring grids at some specific locations), we study the control in clustered graphs. More precisely, we use a block model $(N, N_{clusters}, p_{in}, p_{out})$ to generate random topologies where N is the number of nodes, $N_{clusters}$ is the number of clusters, p_{in} is the probability that two nodes within the same cluster are linked, and p_{out} is the probability that two nodes in two distinct clusters are connected.

Figure 5 displays how the number of drivers evolves with the number of clusters for different values of p_{in} when p_{out} is fixed ($p_{out} = 0.1$). For small values of $p_{in} \sim p_{out}$ clusters are poorly marked, and the connectivity is low. The number of drivers in these conditions is large and increases slowly when the number of clusters augments. As p_{in} increases, the clusters becomes more densely connected such that within a cluster less drivers are required in order to control it. As the number of clusters grows, more drivers are required. For large values of p_{in}, the behavious is more complex. We see indeed that for $p_{in} = 0.9$ and $N_{clusters} = 2$, almost 94% of the nodes are needed for control, but this quantity first decreases with the addition of a few more clusters (71% for $N_{clusters} = 5$), before increasing. This behavior can be explained by the fact that controlling a very dense network requires, in our settings, a very large portion of nodes to be drivers. Controlling one cluster alone thus requires to control almost all nodes within this cluster. Nevertheless, when a relatively small (compared to the number of nodes in the graph) number of clusters are interconnected with a few links, nodes in one cluster are able to control nodes in other clusters to which they are connected. As the number of clusters grows, the global connectivity increases rapidly, such that the number of drivers also rises. We show this behavior in more details in figure 6, where the number of drivers is plotted against p_{in} for $N = 200$ and $N_{clusters} \in$
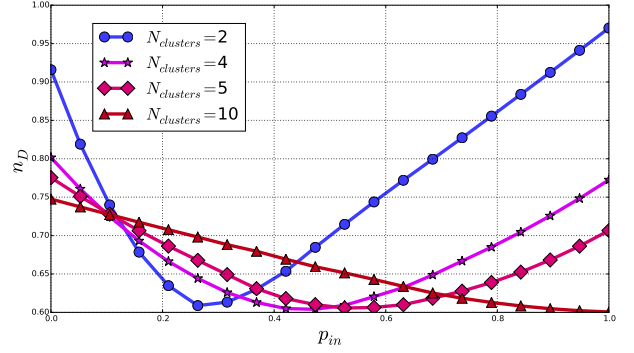
$\{2, 4, 5, 10\}$. For $N_{clusters} = 2$ and $p_{in} = 0.1$ the number of drivers is large since the graph is poorly connected. When p_{in} increases, n_D decreases until a minimum value $n_D \sim 0.6$ at $p_{in} \sim 0.25$. After this point, n_D augments with p_{in}. For $N_{clusters} = 10$, we do not see this behavior : n_D decreases continuously as p_{in} increases as expected from the curves of figure 5.

Until now, we have considered all batteries to be equal, i.e they have the same capacity and charge/discharge rate. Although simple, this assumption might not be verified in practice where different types of batteries exist. Optimizing the locations of different types of storage as to optimize the cost / reliability tradeoff is out of the scope of this paper. Nevertheless, we studied how the number of drivers behaves when the batteries have different capacities. More precisely, we draw the capacities of the batteries from a normal distribution $\mathcal{N}(\mu_\lambda, \sigma_\lambda)$ and keep a simple erdos-renyi topology for the power grid. Note that each node is assigned a capacity regardless of its caracteristics (degree, betweeness, and so on...). In figure 6, we plot n_D as a function of the relative standard deviation of the battery capacity distribution $\sigma_\lambda/\mu_\lambda$. We see that n_D increases with the variance of the capacity distribution for all three gramian based metrics considered. Moreover, this rise is abrupt since n_D goes from 60% for $\frac{\sigma_\lambda}{\mu_\lambda} \sim 0.15$ to 100% for $\frac{\sigma_\lambda}{\mu_\lambda} \sim 0.27$.

Since real power grids topologies are known to be far from random, we consider here, as a real case, the european transmission power grid which topology was obtained from [12]. The network contains 1494 nodes and 2156 edges and spans 25 european countries. A representation of this graph can be found in figure 8 where the nodes are colored according to their country. We select the power distribution and the line capacities randomly, and use the method described above.

We use the trace of the Gramian matrix for the optimization. The top panel of figure 9 shows that the rank of the Gramian increases with the size of the controllers until reaching full rank ($rank[W_S] = 2N_{nodes}$) for $N_D = 1244$. Above this point, we compute the average control energy needed to drive
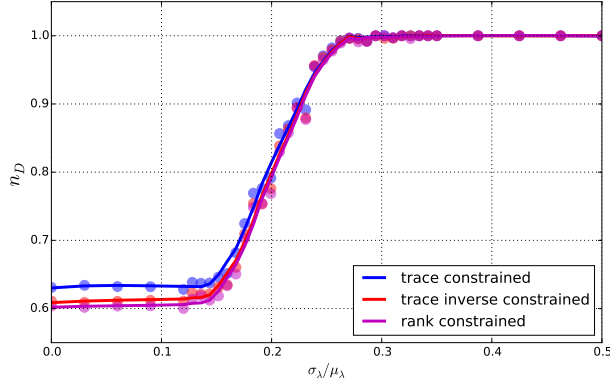
Figure 7: n_D against the relative standard deviation of the capacity distribution of the batteries $\frac{\sigma_\lambda}{\mu_\lambda}$. The dots are averages over 100 realizations and the curves are obtained using a Savitzky-Golay filter, each color shows the results for a given metric. The graphs are erdos-renyi with $N = 100$ and $p = 0.3$, and $\mu_\lambda = 100$ units.
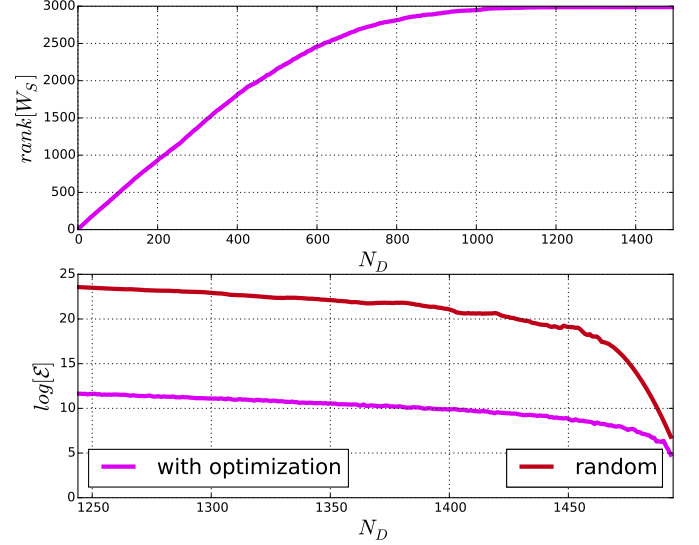

Figure 9: Gramian rank and control energy evolution for european transmission power grid (see figure 8).

Figure 8: European transmission power grid [12]. Nodes are colored according to their county.

the system from an initial random state to a random final state. The curves on the bottom panel of figure 9 show the results for the optimized driver sets and for random driver sets. As can be seen on figure 9, as the size of the driver set increases, the control energy tend to decrease. But, we need less energy with the optimized driver set than with randomly sampled sets.
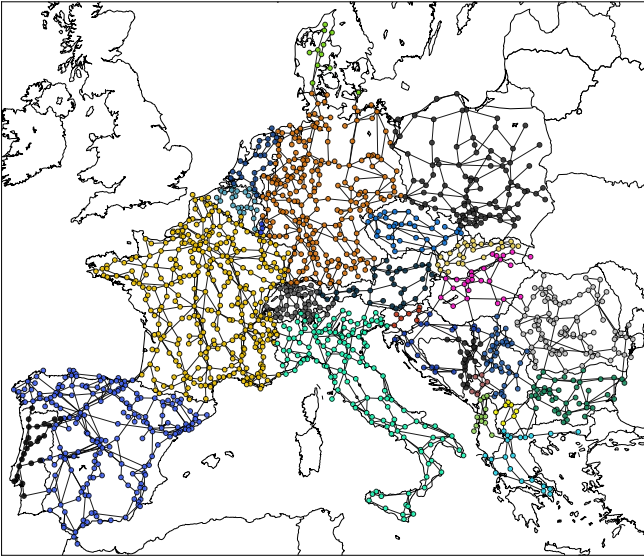
VI. CONCLUSION

In this paper, we considered the case of networks of prosumers which can behave as generators or loads depending on weather conditions. We modeled the grid as a coupled oscillators network and approximated the dynamics with a system of second order linear differencial equations. We seek to control this dynamic when small perturbations occur by placing storage devices at a subset of the nodes. We believe that the energy that should be injected or absorbed from the grid by these controllers should be minimized. Given the diversity of possible situations, we seek the subset of nodes that, on average, necessitates minimum control energy. Based on the gramian matrix of the system and submodular set functions, we show how to find driver sets that use low energy on average and respect the system constraints.

We believe that interesting work could be done by combining this model with real production and consumption data. There are indeed complex spatial and temporal correlations that impacts these distributions. Weather perturbations would therefore affect the nodes not completely at random, and affect how control should be designed.

On the other hand, we seek in this paper, drivers that achieve full control of the system although this might not be needed in practice. More subtle controllability schemes might give better results both in terms of number of drivers and control energy.

REFERENCES

[1] S. D. Ramchurn *et al.*, "Putting the 'smarts' into the smart grid: A grand challenge for artificial intelligence," *Commun. ACM*, vol. 55, no. 4, pp. 86–97, Apr. 2012.

[2] a. J. D. Rathnayaka, V. Potdar, and M. H. Ou, "Prosumer management in socio-technical smart grid," *Proceedings of the CUBE International Information Technology Conference on - CUBE '12*, p. 483, 2012. [Online]. Available: http://dl.acm.org/citation.cfm?doid=2381716.2381808

[3] G. Filatrella, a. H. Nielsen, and N. F. Pedersen, "Analysis of a power grid using a Kuramoto-like model," *The European Physical Journal B*, vol. 61, no. 4, pp. 485–491, mar 2008. [Online]. Available: http://www.springerlink.com/index/10.1140/epjb/e2008-00098-8

[4] Y.-Y. Liu and A.-L. Barabási, "Control Principles of Complex Networks," pp. 1–55, 2015. [Online]. Available: http://arxiv.org/abs/1508.05384

[5] T. Summers, F. Cortesi, and J. Lygeros, "On Submodularity and Controllability in Complex Dynamical Networks," *arXiv preprint arXiv:1404.7665*, pp. 1–10, 2014. [Online]. Available: http://arxiv.org/abs/1404.7665

[6] M. Minoux, "Accelerated greedy algorithms for maximizing submodular set functions," in *Optimization Techniques*, ser. Lecture Notes in Control and Information Sciences, J. Stoer, Ed. Springer Berlin Heidelberg, 1978, vol. 7, pp. 234–243. [Online]. Available: http://dx.doi.org/10.1007/BFb0006528

[7] A. Krause and D. Golovin, "Submodular function maximization," *Tractability: Practical Approaches to Hard Problems*, vol. 3, pp. 71–104, 2014.

[8] C.-T. Lin, "Structural controllability," *IEEE Transactions on Automatic Control*, vol. 19, no. 3, pp. 201–208, Jun 1974.

[9] Z. Yuan, C. Zhao, W. X. Wang, Z. Di, and Y. C. Lai, "Exact controllability of multiplex networks," *New Journal of Physics*, vol. 16, 2014.

[10] G. Yan, J. Ren, Y. C. Lai, C. H. Lai, and B. Li, "Controlling complex networks: How much energy is needed?" *Physical Review Letters*, vol. 108, no. 21, pp. 1–5, 2012.

[11] F. Dörfler, M. Chertkov, and F. Bullo, "Synchronization in complex oscillator networks and smart grids." *Proceedings of the National Academy of Sciences of the United States of America*, vol. 110, no. 6, pp. 2005–2010, 2013. [Online]. Available: http://www.ncbi.nlm.nih.gov/pubmed/23319658

[12] T. V. Jensen, H. de Sevin, M. Greiner, and P. Pinson, "The re-europe data set," Dec. 2015. [Online]. Available: http://dx.doi.org/10.5281/zenodo.35177